

A REVIEW AND TEST OF SHORELINE EXTRACTION TECHNIQUES

R. Angelini¹, E. Angelats², G. Luzi², F. Ribas³, A. Masiero¹, F. Mugnai¹

¹ Department of Civil and Environmental Engineering, University of Florence, Italy - (riccardo.angelini, andrea.masiero, francesco.mugnai)@unifi.it

² Geomatics Research Unit. Department of Signal Theory and Communication (TSC), Centre Tecnològic de Telecomunicacions de Catalunya (CTTC/CERCA) – (guido.luzi, eduard.angelats)@cttc.cat

³ Departament de Física, Universitat Politècnica de Catalunya, Escola d'Enginyeria de Telecomunicació i Aeroespacial de Castelldefels, Mòdul C3, office 116c/ Esteve Terradas 5 E-08860 Castelldefels Catalonia, Spain - francesca.ribas@upc.edu

KEY WORDS: shoreline extraction, classifier, machine learning, multispectral, radar.

ABSTRACT:

Shoreline represents the boundary between land and sea, and its accurate extraction is of utmost importance because of the economic and ecological value of coastal areas. Nowadays, satellite remote sensing is widely used for monitoring the natural environment. Indeed, satellite remote sensing data are cost-effective and periodically available over large areas at a relatively high spatial resolution. Hence, the automatic shoreline extraction from satellite images is a fundamental task for coastal monitoring and management. Shoreline extraction methods are usually applied to satellite remote sensing data. The goal of this study is to compare the performance of different shoreline extraction methods, such as thresholding and more complex classification approaches, such as Random Forest (RF), Minimum Distance (MD), Maximum Likelihood (ML) and K-means, using both optical and radar images. The considered case study area is the shallow basin of the Orbetello Lagoon and one of its ayre called Feniglia. The data supplier is the Copernicus program, which, through the Sentinel-1 and Sentinel-2 missions, provides medium-resolution, open-access products. The accuracy of the obtained results from both methodologies is checked by validating the extracted shoreline using an aerial orthomosaic and, subsequently, a manually extracted shoreline. A preliminary accuracy assessment was performed for image classification, focusing on extracting four classes: water, soil, urban, and forest, using manual segmentation as a reference. In terms of deviation from the reference shoreline, the results obtained through the analysed methodologies achieved an accuracy of 3.75 m, less than half of the pixel size of the Sentinel-1 and Sentinel-2 used products.

1. INTRODUCTION

Coastal environments are vital for their biodiversity and for human activities, both leisure and economic ones. The coastal area represents a highly dynamic system which suffers from continuous and several transformations. The causes of changes in coastal zones can be grouped into geological and geomorphological, hydrodynamic, biological, climatic, and anthropogenic (Łabuz, 2015).

Monitoring the coastal environment is usually conducted by defining several indicators, where the most common and widely used one is the shoreline. The easiest definition of the "shoreline" is the boundary between land and sea (Anders and Byrnes, 1991). However, such high temporal and spatial variability in coastal environments requires a more precise definition of this indicator. According to (Zollini et al., 2020), the shoreline indicators can be divided into three main categories:

- Characteristic visible by an operator on an aerial or remote sensing image;
- The intersection between a tidal datum and a digital terrain model or a coastal profile;
- Characteristics of images identified by automatic algorithms are not necessarily visible to an unaided operator.

The methodology adopted in this paper provides a systematic use of third-type data compared with "ground truth" coming from the first type.

Traditional field data collection, typically manually performed by a human operator over a large coastal area, is usually time-consuming, expensive, and affected by the operator's capacity

and choices (Spinosa et al., 2021a). In contrast, remote sensing has emerged as a valuable tool for coastal monitoring due to its ability to provide large-scale, periodically regular, frequent, and cost-effective data.

Satellite images from both passive and active remote sensors can be used to extract the shoreline. Passive sensors, such as multispectral ones, rely on the natural reflectance properties of coastal features on the considered portion of the electromagnetic spectrum, typically ranging from the visible to the infrared. The optical images provide a simple way to extract shorelines based on the spectral reflectance of both land and water (Demir et al., 2016). Unfortunately, satellite multispectral data are sensitive to weather conditions. Instead, active remote sensing techniques, such as SAR, can allow usable measurement collection independently in the presence of gases and clouds, representing a clear advantage concerning passive sensors (Rozenstein et al., 2016). However, on the other hand, SAR images require more pre-processing steps than optical ones.

Automated methods for shoreline extraction from remote sensing imagery can be grouped into three categories (Toure et al., 2019): thresholding, classification, and edge detection-based approaches.

Thresholding represents the easiest and fastest way in segmentation techniques. However, it may not be sufficiently accurate in some contexts affected by high variability in luminance value. Motivated by this reason, several efforts have been spent in order to improve the thresholding results: designing an optimal threshold, e.g. Otsu's one (Otsu, 1979), proposing more complex and flexible approaches such as adaptive thresholding (Aedla et al., 2015) and multi-threshold (Jishuang and Wang, 2002).

Classification aims at providing a simplified data representation, partitioning data into a collection of uniform regions called classes. Classification methods can be either supervised or unsupervised. Due to its simplicity, k-means is the most widely used unsupervised method (García-Rubio et al., 2015). Supervised classification usually allows for handling more complex phenomena (Tsekouras et al., 2018a). Supervised classifiers like Maximum Likelihood (ML), Random Forest or Minimum Distance (MD) (Bamdadinejad et al., 2021) are pretty commonly used nowadays. Independently of the specifically implemented classifier, robust results can only be obtained when training it with a sufficiently informative and representative dataset, i.e. a supervised classifier, able to work with data from different satellite missions and different beach topologies, should be trained with images taken from different satellites and environments (Abdelhady et al., 2022). Many authors successfully tested the water or vegetation spectral indexes, such as the Normalised Difference Water Index (NDWI) or Normalised Difference Vegetation Index (Ozturk and Sesli, 2015). They can be used both in thresholding and preliminarily in classification methodologies.

Edge detection approaches exploit variations in colour, grey-level intensities or texture of an image to determine the borders of the area of interest, i.e. the shoreline. Many authors proposed different approaches using Canny Edge detection (Tonye et al., 2000), Snakes (Klinger et al., 2011) and Level Set Algorithm (Ouyang et al., 2010).

Most of the above-mentioned approaches have been implemented for passive sensor data (e.g., multispectral), few for active ones, and probably even fewer efforts have been spent on combining the two. Motivated by the above observation, this study aims to compare different strategies to extract the shoreline from radar and multispectral images. In particular, this work is focused on comparing thresholding and supervised and unsupervised classification methods.

The considered methods are tested on Sentinel-1 Synthetic Aperture Radar (SAR) images and Sentinel-2 Multispectral Instrument (MSI) images at 10m of spatial resolution. The testing area is the Feniglia coast, a 6km ayre portion of the coast on the Orbetello Lagoon system, located in Tuscany (Italy). The accuracy of the obtained results is checked by validating the extracted shoreline using a hand-made one derived from an aerial orthomosaic provided by Tuscany Region WMS. The classification accuracy was estimated using a ground truth by visual interpretation of the image classes.

2. STUDY AREA

The testing area is situated in the south of Tuscany region in Italy. It involves the Orbetello lagoon and one of its two spits called Feniglia, formed by sea level rise during the Holocene and diffraction of the sea waves through Monte Argentario Island, now connected to the mainland (Barnes, 1980). Feniglia spit includes a 6-km-long beach with an associated protected area established in 1971. In addition to being a natural reserve, it represents an area of great economic (touristic) interest. In the past, some research works have already identified shoreline modification trends, the presence of mega-cusps (Cipriani et al., 2004) and the evolution of vegetated surface (Bellarosa et al., 1996) on the Feniglia beach. Given the accelerating climate changes and sea level rise, new studies are required.



Figure 1: The testing area. Feniglia is the spit on the south of the lagoon visible in the figure. The map is shown in WGS84-UTM32 (in meters).

3. MATERIAL AND METHODOLOGY

This section aims at presenting data (subsection 3.1) and methods used in this work, i.e. thresholding (subsection 3.2) and image classification techniques (subsection 3.3). Both optical and radar open-source data sources have been used and obtained thanks to the Copernicus program. Furthermore, open-source software was employed for data processing, i.e. Sentinel Application Platform (SNAP) and QGIS 3.4.

3.1 Data Sources

A multispectral Sentinel-2 satellite image and a SAR Sentinel-1 satellite image were used in this study, as shown in Table 1. Sentinel-1 and 2 are satellite missions developed by the European Space Agency (ESA) as part of the Copernicus Programme, differing in particular for the sensors mounted on the corresponding satellites. Satellite data are freely available at different processing levels in both cases. Data have been downloaded from the Copernicus Open Access Hub website.

Satellite	Date [dd/mm/yyyy]	Time [hh:mm]	Tide [m]	Wave [m]
S-2	23/07/2019	10:10	0.01	0.31
S-1	18/07/2019	05:19	0.07	0.43
Ortho	19/07/2019	12:15	0.08	0.41

Table 1. Images used in this study with framework conditions.

Sentinel-2 satellites are equipped with a Multispectral Imager (MSI) that captures images in 13 spectral bands, including visible, near-infrared and shortwave infrared. The spatial resolution of the image ranges from 10 to 60 meters, depending on the spectral band. In this study, Level-2A products of Sentinel-2 have been used, i.e., data including orthorectification, atmospheric corrections and cloud masking.

Sentinel-1 mission provides different acquisition modes. In this work, the radar image was downloaded in Interferometric Wide Swath (IW) acquisition mode, which provides 250 km of image swath and 5 m x 20 m spatial resolution. Then, a Ground Range Detected (GRD) product was selected. GRD products consist of focused SAR data that have been detected, multi-looked and

projected to ground range using the Earth ellipsoid model WGS84, with approximately 10 m x 10 m resolution cells and square pixel spacing.

In our current implementation of the considered methods, Sentinel-1 and Sentinel-2 data have been used separately to extract the shoreline. Nevertheless, our future investigation will also be dedicated to improving the shoreline extraction results by properly fusing their information.

In order to make some assessments on the performance of the implemented methods, an orthomosaic, with 0.2 m x 0.2 m spatial resolution provided by Tuscany region, is used for comparison with the satellite data.

Oceanographic data, such as wave and tidal information, are essential in coastal applications such as shoreline extraction. This is because the position of the shoreline changes continuously and can be affected by tidal cycles and wave-induced variations. In addition, using data from nearby stations can improve the accuracy of shoreline detection by accounting for local conditions such as tides and wave heights, especially in complex coastal environments (Liu et al., 2016).

Wave and tide data from the Giannutri buoy, managed by the Tuscany region, and the Civitavecchia tide gauge, managed by Istituto Superiore per la Protezione e la Ricerca Ambientale (ISPRA), were considered in the analysis as the closest gauges to the examination site. However, the data with small oscillations were excluded in the following step. It should be noted that this study focused on the strategies for extracting the shoreline and not on temporal or instantaneous monitoring. Therefore, it was possible to select data that were temporally sufficiently close to each other.

3.2 Thresholding

The details of the adopted thresholding methodology are presented in the flowchart shown in Figure 2. Sentinel-2 imagery was downloaded at level 2A, an orthoimage atmospherically corrected Surface Reflectance product. NDWI was calculated on the area of interest using the following formula:

$$NDWI = \frac{B3 - B8}{B3 + B8} \quad (1)$$

where $B3$ = green band
 $B8$ = Near Infrared band

Due to the nature of SAR data, the shoreline extraction process on the Sentinel-1 radar image included the following pre-processing steps, performed with the open-source SNAP software provided by ESA:

- Use the orbit file to correct the satellite orbit deviations and clock errors.
- Thermal noise removal: this step removes the effect of electronic noise generated by the radar receiver.
- Calibration: this step corrects the signal's amplitude and reduces the effect of errors in the measurement/acquisition system.
- Speckle filter: this step reduces the speckle noise generated by the radar beam's interaction with the

Earth's rough surface. The Lee Filter was used because of its effectiveness for feature extraction, i.e. its application preserves edge information while suppressing speckle noise (Sun et al., 2016).

- Terrain correction: this step corrects the distortions in the image due to the topography of the Earth's surface. The image was geocoded in the WGS-84 UTM-32N reference system using the SRTM digital terrain model.



Figure 2: NDWI value along a transect. The red dot represents the value of NDWI used to separate land and water.

Different polarisations and window sizes were used for the Lee speckle filter. The following ones have been chosen for comparison:

- VH polarisation with Lee Filter 7mx7m
- VV polarisation with Lee Filter 7mx7m
- VV polarisation with Lee Filter 5mx5m

The threshold chosen to binarize the SAR image in a particular sandy beach environment was set to -20dB, in accordance with (Chen et al., 2022).

Instead, the land/water separation in the raster image representing NDWI was obtained by setting a threshold value of 0, according to (Ouma and Tateishi, 2006), to separate water and land areas.

The resulting images from radar and multispectral analysis were vectorised, as a line format and smoothed in QGIS to improve the quality of the obtained vector, as shown in the diagram of Figure 3.

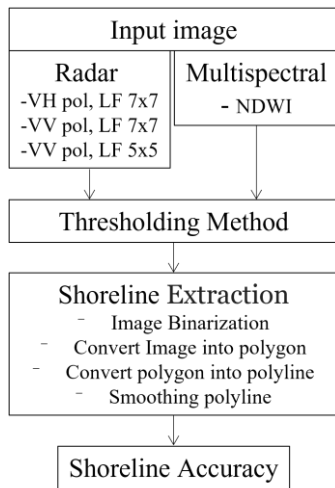


Figure 3: Diagram of thresholding methodology in shoreline extraction.

3.3 Classification Methods

The considered classification methods for shoreline extraction have been implemented in SNAP software. Both radar and multispectral images are used to test different approaches, and different methods to enhance spectral differences in the images are also tested. Regarding radar data, the absolute value of VH polarisation multiplied by VV polarisation was calculated. Concerning the optical data, NDWI spectral index and different band combinations were tested.

The methodology for extracting the shoreline after image classification is shown in Figure 4. Classification strategies can be divided into different categories depending on the following:

- whether the classification is pixel-based or object-oriented,
- if it is supervised or unsupervised.

In this work, Maximum Likelihood, Minimum Distance and Random Forest are tested as supervised methods. Instead, K-means was deployed for the unsupervised case. Processing steps following the classification one, i.e. from "Shoreline Extraction", are similar to those already described in subsection 3.2.

3.3.1 Maximum Likelihood (ML)

The maximum likelihood classifier is a widely used method for image classification, where pixel classes are assigned based on the highest likelihood criterion. The separation between the classes in the decision space is one of the main factors impacting ML-based classification accuracy (Ahmad and Quegan, 2012). ML has been successfully used to detect temporal shoreline changes (Tamassoki et al., 2014).

3.3.2 Minimum Distance (MD)

The minimum distance classifier is based on the availability of central class values (e.g. means, determined in the training phase): pixel categories are determined as those ensuring the minimum distance for each central class value (B. R. Shivakumar and S. V. Rajashekararadhya, 2017). This method is often used in remote sensing and image analysis applications thanks to its simplicity and efficiency in classification tasks.

3.3.3 Random Forest (RF)

Random forest (RF) is a popular machine learning method that generates a large group, or forest, of classification and regression trees by randomly and iteratively sampling data and variables. The RF classification output represents the statistical mode of many decision trees, which leads to a more robust model than a single classification tree produced by a single model run (Breiman, 2001). In the regression case, RF output represents the average of all the regression trees grown in parallel without pruning. RF has several valuable properties, including internal error estimates, the ability to estimate variable importance, and the capability to handle weak explanatory variables. Considering the coastal area classification problem, good results were obtained using the RF classifier with input data that contained the NIR band (Dizaji, 2018).

3.3.4 K-means

K-means assigns each pixel in the scene to the nearest cluster centre, which is determined as the mean value of all the samples belonging to the cluster. Its simplicity and computational efficiency make it a popular choice for clustering large datasets. However, it does not consider data scale variations and correlations. Furthermore, it minimises the intra-cluster variance, but reaching a global minimum is not guaranteed. Despite these drawbacks, it is one of the most common cluster analysis choices.

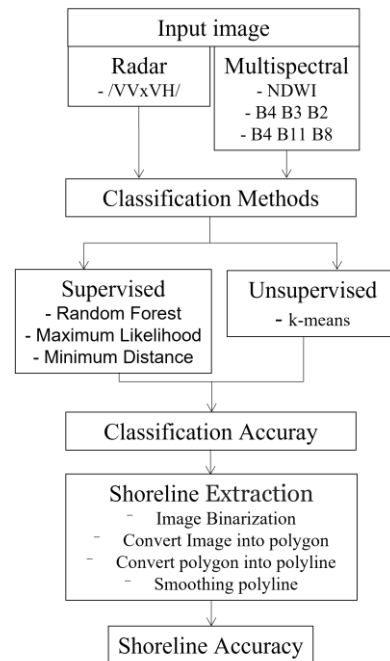


Figure 4: Diagram of classification methodology in shoreline extraction.

3.3.5 Classification Accuracy Assessment

Accuracy assessment was obtained by comparing the outcomes of the considered methods with a manually performed classification. The common way to report spatial errors is through the *confusion matrix*, which reveals the misclassifications for each group. The error matrix is always presented as a square matrix, and the confusion matrix diagonal elements indicate the number of correctly classified samples. Instead, the off-diagonal

elements provide details about omission and commission errors. The criterion for defining accuracy chosen was overall accuracy (OA), defined by summing the number of correctly classified values and dividing by the total number of samples.

$$OA = \frac{(TP+TN)}{(TP+FP+TN+FN)} \quad (2)$$

Table 2 shows the classification results of some of the examined combinations of supervised methods and variables chosen for subsequent shoreline extraction. Figure 5 compares the classification results on S1 data in certain of the considered cases.

Mission	Input data	Method	OA
S1	/VVxVH/	ML	0.852
S1	/VVxVH/	MD	0.847
S1	/VVxVH/	RF	0.847
S2	NDWI	ML	0.169
S2	NDWI	MD	0.169
S2	NDWI	RF	0.169

Table 2. Classification accuracy in terms of Overall Accuracy (OA).

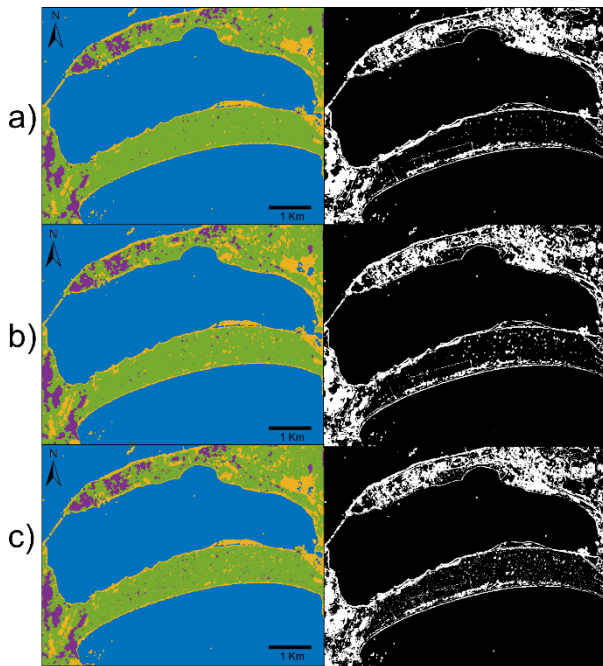


Figure 5: Classification results (left column) on S1 data and the corresponding wrongly classified pixels (right column) for a) MD on /VVxVH/ band, b) ML on /VVxVH/ band, c) RF on /VVxVH/ band. Considered classes: forest (green), urban (purple), water (blue), and soil (yellow).

4. RESULTS AND DISCUSSION

A geometric comparison between the determined shorelines was conducted by comparing them with one manually extracted from the high-resolution orthomosaic mentioned in Section 3.1. The method described in (Demir et al., 2017) has been implemented in a GIS environment to obtain a fair accuracy estimation of the

shoreline extraction performance and is quite commonly well accepted in the literature. Each extracted shoreline was sampled every 10 m for about 600 points. Subsequently, transects were generated by measuring the Euclidean distance between the extracted shorelines and the manually digitised shoreline, as shown in Figure 6.



Fig. 6: Accuracy evaluation of shoreline

Statistical parameters, including minimum, maximum, mean distance, and standard deviation, were calculated to evaluate the results of the two methodologies. The results are reported in Table 3.

Thresholding					
		Min dis [m]	Max dis [m]	Avg dis [m]	Std [m]
S1	VH LF 7x7	0.08	73.76	24.66	11.14
	VV LF 7x7	0.00	44.47	7.82	6.49
	VV LF 5x5	0.02	34.00	7.77	6.21
S2	NDWI	0.02	20.59	6.97	3.95
Classification					
		Min dis [m]	Max dis [m]	Avg dis [m]	Std [m]
S1 /VVxVH/	K-means	0.04	24.66	7.55	5.16
	RF	0.01	25.86	9.00	5.51
	ML	0.02	29.04	11.67	5.80
	MD	0.01	25.23	8.81	5.45
S2 B4B3B2	K-means	0.05	17.94	6.24	3.34
S2 B4B8B11		0.08	15.46	3.75	2.65
S2 NDWI	RF	0.02	20.32	4.95	3.13
	ML	0.02	20.32	4.95	3.13
	MD	0.02	20.32	4.95	3.13

Table 3. Statistical results were derived from distance measurements between the automatically estimated and the manually extracted reference shoreline.

The results demonstrate that the unsupervised k-means classification algorithm, applied to the optical input data with the B4-B8-B11 band combination, achieved the best performance. Additionally, the NDWI index proved to be a valuable input for optical data analysis. Regarding the S1 data, k-means applied to the combination of polarisations composed by an absolute multiplication value between VV and VH resulted in the best performance. The mentioned combinations of bands, sensors, and methodologies achieved a remarkable sub-pixel accuracy.

A comparison was organised in three sectors, each about 2 Km long, along the Feniglia beach, based on the average distance from the reference shoreline, to assess the spatial distribution of these differences. (Figure 5).

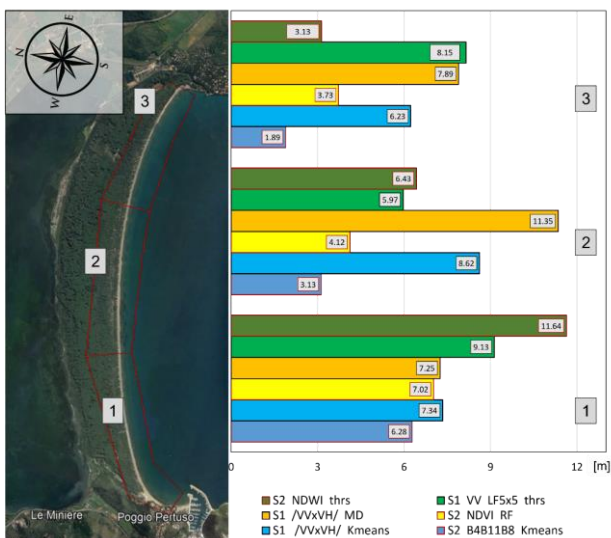


Figure 5: Spatial distribution of the extracted shorelines' mean distance from the reference one.

A careful analysis of the results reveals an accuracy improvement when moving from west to east, from sector 1 to sector 3. This pattern was detected in all the analyses conducted using optical data, whereas the radar performance shows a higher variability and not such a trend behaviour. A possible explanation of the optical trend, which requires further investigation, could be related to the slight increase in beach slope and grain size when moving from sector 1 to sector 3.

The selected study area proved to be very challenging due to the low beach width, which varies between 10 and 50 meters, a size comparable to the satellite image pixel size. Another aspect to consider is the low beach slope. Shoreline detection with the proposed method may be challenging in intertidal areas, where the porous medium is characterised by a higher saturation degree, leading to uncertainties in shoreline detection (Spinosa et al., 2021b). A significant factor in such uncertainties is the reflectance, which in the higher moisture content environment is similar to the water one. In fact, at saturation, the optical path length in water is at its maximum and specific wavelengths may be absorbed entirely (Nolet et al., 2014). Another aspect to consider for improving the analyses in this environment is fully accounting for the run-up differences caused by waves and tides. To extend the methodology to other areas, it is also necessary to

consider the varying grain sizes present in different sandy beaches.

Regarding the threshold methodology, improvements can be obtained by applying segmentation algorithms, such as locally adaptive thresholding algorithms, which can enhance the land/water boundary recognition and thus reduce the discontinuity of coastal edges that can occur in low contrast areas in the image (Liu and Jezek, 2004). As for classification methods, in the unsupervised case, Principal Component Analysis (PCA) may be used for an ad hoc determination of the number of classes (Hannv et al., 2013). Regarding supervised methods, thanks to their strong capability to handle complex phenomena, neural networks could improve coastline detection accuracy (Tsekouras et al., 2018b).

5. CONCLUSIONS

The importance of shoreline extraction as a field of study lies in its relevance to environmental and socioeconomic issues. Coastal erosion, sea level rise, and coastal land use and development are just a few examples of applications where accurate shoreline extraction is crucial.

In this work, different methods of shoreline extraction from satellite imagery, both radar and multispectral, were implemented. Thresholding methodology in water/soil distinction and later image classification strategies were tested. The accuracy of both methodologies was evaluated using a high-resolution orthophoto as ground truth. In addition, the accuracy of the image classification was also evaluated using a ground truth built through manual classification. This allowed for a more comprehensive evaluation of the accuracy of the methodologies and provided additional validation of the results. Both methods achieved subpixel levels of accuracy. The achieved result is remarkable, given the complexity of the area under examination.

The methodologies implemented in this study have the advantage of being executable with free software and data and reproducible in different scenarios.

The advantages of using satellite imagery for shoreline extraction include its ability to cover large areas at a low cost compared to traditional methods, such as aerial photography and field surveys. The proposed methodology has the advantage of being adaptable to optical and radar data, which can be used complementarily. Among the possible future developments, data fusion techniques and Machine learning algorithms can also be used to improve the accuracy and efficiency of shoreline extraction.

REFERENCES

- Abdelhady, H.U., Troy, C.D., Habib, A., Manish, R., 2022. A Simple, Fully Automated Shoreline Detection Algorithm for High-Resolution Multi-Spectral Imagery. *Remote Sens.* 14, 557. <https://doi.org/10.3390/rs14030557>
- Aedla, R., Dwarakish, G.S., Reddy, D.V., 2015. Automatic Shoreline Detection and Change Detection Analysis of Netravati-GurpurRivermouth Using Histogram Equalization and Adaptive Thresholding Techniques. *Aquat. Procedia, INTERNATIONAL CONFERENCE ON WATER RESOURCES, COASTAL AND OCEAN ENGINEERING (ICWRCOE'15)* 4, 563–570. <https://doi.org/10.1016/j.aqpro.2015.02.073>

- Ahmad, A., Quegan, S., 2012. Analysis of maximum likelihood classification on multispectral data. *Appl. Math. Sci.* 6, 6425–6436.
- Anders, F.J., Byrnes, M., 1991. Accuracy of shoreline change rates as determined from maps and aerial photographs. *Shore Beach* 59, 17–26.
- B R, Shivakumar., S V, Rajashekaradhyaa., 2017. Spectral Similarity for Evaluating Classification Performance of Traditional Classifiers. <https://doi.org/10.1109/WiSPNET.2017.8300111>
- Bamdadinejad, M., Ketabdari, M.J., Chavooshi, S.M.H., 2021. Shoreline Extraction Using Image Processing of Satellite Imageries. *J. Indian Soc. Remote Sens.* 49, 2365–2375. <https://doi.org/10.1007/s12524-021-01398-3>
- Barnes, R.S.K., 1980. *Coastal Lagoons*. CUP Archive.
- Bellarosa, R., Codipietro, P., Piovesan, G., Schirone, B., 1996. Degradation, rehabilitation and sustainable management of a dunal ecosystem in central Italy. *Land Degrad. Dev.* 7, 297–311. [https://doi.org/10.1002/\(SICI\)1099-145X\(199612\)7:4<297::AID-LDR235>3.0.CO;2-M](https://doi.org/10.1002/(SICI)1099-145X(199612)7:4<297::AID-LDR235>3.0.CO;2-M)
- Breiman, L., 2001. Random Forests. *Mach. Learn.* 45, 5–32. <https://doi.org/10.1023/A:1010933404324>
- Chen, C., Chen, H., Liang, J., Huang, W., Xu, W., Li, B., Wang, J., 2022. Extraction of Water Body Information from Remote Sensing Imagery While Considering Greenness and Wetness Based on Tasseled Cap Transformation. *Remote Sens.* 14, 3001. <https://doi.org/10.3390/rs14133001>
- Cipriani, L.E., Ferri, S., Iannotta, P., Mannori, S., Pranzini, E., 2004. Evoluzione recente delle spiagge toscane. *Erosione Costiera* 75–92.
- Demir, N., Kaynarca, M., Oy, S., 2016. EXTRACTION OF COASTLINES WITH FUZZY APPROACH USING SENTINEL-1 SAR IMAGE. *ISPRS - Int. Arch. Photogramm. Remote Sens. Spat. Inf. Sci.* XLI-B7, 747–751. <https://doi.org/10.5194/isprs-archives-XLI-B7-747-2016>
- Demir, N., Oy, S., Erdem, F., Şeker, D.Z., Bayram, B., 2017. INTEGRATED SHORELINE EXTRACTION APPROACH WITH USE OF RASAT MS AND SENTINEL-1A SAR IMAGES. *ISPRS Ann. Photogramm. Remote Sens. Spat. Inf. Sci.* IV-2-W4, 445–449. <https://doi.org/10.5194/isprs-annals-IV-2-W4-445-2017>
- Dizaji, R., 2018. Coastline Extraction By Using Random Forest Method; A Case Study Of Istanbul. *Geomatik.* <https://doi.org/10.29128/geomatik.362179>
- García-Rubio, G., Huntley, D., Russell, P., 2015. Evaluating shoreline identification using optical satellite images. *Mar. Geol.* 359, 96–105. <https://doi.org/10.1016/j.margeo.2014.11.002>
- Hannv, Z., Qigang, J., Jiang, X., 2013. Coastline Extraction Using Support Vector Machine from Remote Sensing Image. *J. Multimed.* 8, 175–182. <https://doi.org/10.4304/jmm.8.2.175-182>
- Jishuang, Q., Wang, C., 2002. A MULTI-THRESHOLD BASED MORPHOLOGICAL APPROACH FOR EXTRACTING COASTAL LINE FEATURE IN REMOTE SENSED IMAGES. *Klinger, T., Ziems, M., Heipke, C., Schenke, H.W., Ott, N., 2011. Antarctic Coastline Detection using Snakes. Photogramm. - Fernerkund. - Geoinformation* 421–434. <https://doi.org/10.1127/1432-8364/2011/0095>
- Łabuz, T.A., 2015. Environmental Impacts—Coastal Erosion and Coastline Changes, in: *The BACC II Author Team (Ed.), Second Assessment of Climate Change for the Baltic Sea Basin, Regional Climate Studies*. Springer International Publishing, Cham, pp. 381–396. https://doi.org/10.1007/978-3-319-16006-1_20
- Liu, H., Jezek, K.C., 2004. Automated extraction of coastline from satellite imagery by integrating Canny edge detection and locally adaptive thresholding methods. *Int. J. Remote Sens.* 25, 937–958. <https://doi.org/10.1080/0143116031000139890>
- Liu, Z., Li, F., Li, N., Zhang, H., 2016. A Novel Region-Merging Approach for Coastline Extraction From Sentinel-1A IW Mode SAR Imagery. *IEEE Geosci. Remote Sens. Lett.* <https://doi.org/10.1109/LGRS.2015.2510745>
- Nolet, C., Poortinga, A., Roosjen, P., Bartholomeus, H., Ruessink, G., 2014. Measuring and Modeling the Effect of Surface Moisture on the Spectral Reflectance of Coastal Beach Sand. *PLOS ONE* 9, e112151. <https://doi.org/10.1371/journal.pone.0112151>
- Otsu, N., 1979. A Threshold Selection Method from Gray-Level Histograms. *IEEE Trans. Syst. Man Cybern.* 9, 62–66. <https://doi.org/10.1109/TSMC.1979.4310076>
- Ouma, Y.O., Tateishi, R., 2006. A water index for rapid mapping of shoreline changes of five East African Rift Valley lakes: an empirical analysis using Landsat TM and ETM+ data. *Int. J. Remote Sens.* 27, 3153–3181. <https://doi.org/10.1080/01431160500309934>
- Ouyang, Y., Chong, J., Wu, Y., 2010. Two coastline detection methods in Synthetic Aperture Radar imagery based on Level Set Algorithm. *Int. J. Remote Sens.* 31, 4957–4968. <https://doi.org/10.1080/01431161.2010.485142>
- Ozturk, D., Sesli, F.A., 2015. Shoreline change analysis of the Kizilirmak Lagoon Series. *Ocean Coast. Manag., Special Issue: Third International Symposium on Integrated Coastal Zone Management (ICZM): Towards Sustainable Coasts - “Recent developments and advancements”* 118, 290–308. <https://doi.org/10.1016/j.ocecoaman.2015.03.009>
- Rozenstein, O., Siegal, Z., Blumberg, D., Adamowski, J., 2016. Investigating the backscatter contrast anomaly in synthetic aperture radar (SAR) imagery of the dunes along the Israel–Egypt border. *Int. J. Appl. Earth Obs. Geoinformation* 46, 13–21. <https://doi.org/10.1016/j.jag.2015.11.008>
- Spinosa, A., Ziemba, A., Saponieri, A., Damiani, L., El Serafy, G., 2021a. Remote Sensing-Based Automatic Detection of Shoreline Position: A Case Study in Apulia Region. *J. Mar. Sci. Eng.* 9, 575. <https://doi.org/10.3390/jmse9060575>
- Sun, S., Liu, R., Yang, C., Zhou, H.B., Zhao, J., Ma, J., 2016. A Comparative Study on the Speckle Filters for the Very High Resolution Polarimetric Synthetic Aperture Radar Imagery. *J. Appl. Remote Sens.* 10. <https://doi.org/10.1117/1.JRS.10.045014>

Tamassoki, E., Amiri, H., Soleymani, Z., 2014. Monitoring of shoreline changes using remote sensing (case study: coastal city of Bandar Abbas). *IOP Conf. Ser. Earth Environ. Sci.* 20, 012023. <https://doi.org/10.1088/1755-1315/20/1/012023>

Tonye, E., Akono, A., Nyongui, A., Nlend, C., Rudant, J.-P., 2000. Cartographie des traits de côte par analyse texturale d'images radar à synthèse d'ouverture ERS-1 et E-SAR. *Teledetection* 3, 183–204.

Toure, S., Diop, O., Kpalma, K., Maiga, A.S., 2019. Shoreline Detection using Optical Remote Sensing: A Review. *ISPRS Int. J. Geo-Inf.* 8, 75. <https://doi.org/10.3390/ijgi8020075>

Tsekouras, G.E., Trygonis, V., Maniatopoulos, A., Rigos, A., Chatzipavlis, A., Tsimikas, J., Mitianoudis, N., Velegrakis, A.F., 2018a. A Hermite neural network incorporating artificial bee colony optimization to model shoreline realignment at a reef-fronted beach. *Neurocomputing, Applications of Neural Modeling in the new era for data and IT* 280, 32–45. <https://doi.org/10.1016/j.neucom.2017.07.070>

Tsekouras, G.E., Trygonis, V., Maniatopoulos, A., Rigos, A., Chatzipavlis, A., Tsimikas, J., Mitianoudis, N., Velegrakis, A.F., 2018b. A Hermite neural network incorporating artificial bee colony optimization to model shoreline realignment at a reef-fronted beach. *Neurocomputing, Applications of Neural Modeling in the new era for data and IT* 280, 32–45. <https://doi.org/10.1016/j.neucom.2017.07.070>

Zollini, S., Alicandro, M., Cuevas-González, M., Baiocchi, V., Dominici, D., Buscema, P.M., 2020. Shoreline Extraction Based on an Active Connection Matrix (ACM) Image Enhancement Strategy. *J. Mar. Sci. Eng.* 8, 9. <https://doi.org/10.3390/jmse8010009>